Automated Wing Internal Structure Placement Guided by Finite Element Analysis

Justin L. Clough* and Assad A. Oberai†
University of Southern California, Los Angeles, CA, 90089

Andrew J. Zakrajsek‡
AFRL/RQHV, Wright-Patterson AFB, Dayton, OH, 45433

The global structural design layout is typically missing in the early conceptual phase of aircraft design; the internal structure itself is usually left uninitialized until the external geometry of the vehicle is finished. This can lead to errors in the predicted performance of the aircraft. This work details and demonstrates a program, GRASP, which automatically determines the optimal structural layout of traditional components (ribs and spars) for use in this early design stage. A user needed to only provide a wing outer mold line, material properties, vehicle weight, and allowable wing tip deflection. A branch-and-cut style algorithm was implemented to explore the design space of possible rib and spar configurations. For each configuration, a design flow of parametric geometry creation, discretization, and finite element analysis was performed automatically using all open source software packages. This was demonstrated for a wing and other parameters representative of the X-15 aeroplane. The GRASP program calculated a optimal initial design layout of 5 ribs and 2 spars in 139 minutes; it evaluated a total of 11 different configurations and successively selected the one which lowered wing tip deflection. Future work includes adding a more representative loading conditions to match those seen in flight and methods to decrease program run time.

Nomenclature

GRASP = Guided Rib And Spar Placement
MER = Mass Estimating Relations
FE = Finite Element
AM = Additive Manufacturing
OML = Outer Mold Line
ESP = Engineering Sketch Pad

Introduction

The conceptual design of modern aerospace systems is grounded in various multi-disciplinary design processes. These conceptual designs typically focus on the aerodynamic performance, weight assumptions, trajectory analysis, and overall ability of the system to meet the design requirements. A key discipline missing from the majority of early conceptual design, is the global structural design. This is due to the complex nature and knowledge required to design the internal structural layout of a new aerospace system [1–3]. Compounding this complexity is the ever changing vehicle geometry during the conceptual design phase, mainly due to recent advances in parametric geometry. Due to the early design fluidity, the conceptual structural design has been mainly incorporated in design loops through material selection and the resulting empirical Mass Estimating Relations (MERs) [1]. These relations are used until the conceptual design is nearly finalized, which then initializes the structural design. The structural design typically starts with rough hand calculations, up to Finite Element (FE) methods, and eventual structural testing. At this point in the design cycle it is typically too late to greatly affect the overall system design [2]. Therefore, the final conceptual

---

*PhD Student, Aerospace and Mechanical Engineering Department, 854 Downey Way, RRB 101.
†Professor, Aerospace and Mechanical Engineering Department, 854 Downey Way, RRB 101.
‡Research Engineer, Air Force Research Laboratory, AFRL/RQ Bldg. 45, 2130 Eighth Street, Wright-Patterson AFB, OH 45433.

design can complicate the structural design and result in increased weight or reduced efficiency of the system. The early incorporation of structural design is important for understanding the proposed system's feasibility, generating accurate weight predictions, assisting the multi-disciplinary design trade space exploration, and guiding the system to an optimal solution.

To generate rapid conceptual design trades, the structural layout and design should mainly be automated at the conceptual level. Automated structural design and layout has mainly been researched in two separate thrusts: (1) topology optimization, and (2) automated conventional structural optimization and layout. Advanced topology methods have been shown to produce optimal internal geometries with respect to minimizing stress, weight, and other key variables [4, 5]. While this research does show future benefit for the aerospace industry, it is also directly coupled to the current state of Additive Manufacturing (AM). A few of the top research challenges for AM when focused on aerospace system structures are: understanding and predicting damage, machine to machine variability, print scale limitations, and cost of AM [6–8]. Until these areas of research are better understood, AM is not currently a viable solution for traditional aerospace structures. With this understanding, this work focused on the near-term, benefits of automating the structural layout process and incorporating the results early in the conceptual design. While the automated structural layout can be considered a form of topology optimization, it will only be denoted as automated layout throughout this work.

Automating the structural layout process requires a specific and detailed focus on the design geometry, in addition to the selection of a structural analysis method. Recent research is focusing on incorporating structural design earlier in the design loop through automated hand calculation methods [1]. This is aimed at incorporating initial structural design early in the design loop without the need for structural expertise. Adding to this other research has suggested that due to increased computational power, the inclusion of FE method is possible early in conceptual design loop [9]. There are benefits from incorporating the more detailed FE analysis early in the design loop, however, this also introduces new challenges, like automatic mesh generation. This issue is mainly addressed within the design framework. A structural optimization method was completed using FE analysis, automatic mesh generation, and a framework (python) environment [10]. The framework becomes extremely important for the incorporation of the structural design in the multi-disciplinary conceptual design loop. As the design and geometry change the structural design needs to adapt and change. This can be completed using parametric geometry, so the FE method and structural layout update as the vehicle design updates [11]. Using geometry as the center of an automated parametric design loop showed to be an important step for linking the structural design within the conceptual design loop [12, 13]. Therefore, to truly bring automated structural design and placement early in the design loop, there needs to be a focus on common design geometry across disciplines and a framework capable of FE analysis. This leads to the ability to take a conceptual Outer Mold Line (OML) to an initial structural layout without the structural designer in the loop.

Completing the automatic structural layout at a conceptual level requires design knowledge held by structural experts. The vast majority of research in this area has looked at automatically laying out the structure by manually specifying the number of supports throughout the structure. This method still requires an engineer in the loop during the conceptual design. The manual layout of the initial structure for the conceptual design takes time, however, needs to be completed to allow a starting point for the FE analysis. For this work an initial structural placement will be completed using a branch-and-cut style algorithm [14]. This will work to initialize the structural design and allow varying internal automated layouts to take place. The selection of the final automated layout can be performed following design constraints and objectives similar to topology optimization (minimize stress, etc.). Therefore, an OML can be entered into the loop, and the structural design model can continue to add supports while analyzing the structure to finalize an initial solution. Eventually, the goal would be to add an element of knowledge-based conceptual and preliminary structural design practices to this placement model [15–17]. While this is outside the work presented here, this area can become extremely beneficial for future conceptual structural designs as an ability to acquire a faster and higher fidelity automated conceptual structural design.

The work presented here has the goal of highlighting the most advantageous method to achieve early automated structural conceptual designs, within the multi-disciplinary design loop independent of direct structural designer expertise. To accomplish this the automated layout process needs an OML input, design loads, and objective (i.e., minimize wing deflection below an allowable amount). The automation framework then should be linked to the same parametric geometry engine, a layout generation method, FE analysis, and a tailorable framework. The resulting work highlights how an automated conceptual design framework was setup to automate a structure layout without any input from the structural designer.

Methods

The goal was to develop an automated workflow to solve an optimal parametric structural layout problem. In this problem, a user specifies a design constraint that must be satisfied, and a set of integer parameters that define the geometry of the structure. The goal is to find an optimal value of these parameters that would achieve the design constraint. In the specific problem considered, the design constraint is a bound on the maximum allowable tip deflection of a wing under a prescribed loading, the integer parameters are the number of ribs and spars in the wing, and the goal is to find the smallest number of spars and ribs that would achieve the tip-deflection constraint.

In order to solve this problem, the workflow described in Figure 2 was developed. Here the first portion is a geometry creation component, which given the value of the parameters of interest, generates the geometry of the structure. The second component further processes this geometry and generates a FE mesh for it. The third component uses this mesh to solve a structural analysis problem and evaluates the value of the design constraint. Once this workflow is established, it may be used to solve the optimal structural design problem using an appropriate integer programming algorithm. Since the focus of this paper is to demonstrate how this workflow can be established, a simple integer optimization algorithm, that is the branch-and-cut method, was used to solve this problem [14]. This algorithm proceeds as follows:

1) Start with an initial configuration that does not satisfy the design constraint.
2) Increment each integer parameter by 1, and use the workflow to generate multiple designs and to determine the design constraint for each design.
3) If the design constraint is satisfied by one or more designs, the problem is solved.
4) If no design satisfies the constraint, select the one that provided the largest drop in the constraint, and go to Step 2.

The different configurations formed the nodes of a tree which was traversed in a depth-first manner. An example of this tree is shown in Figure 1.
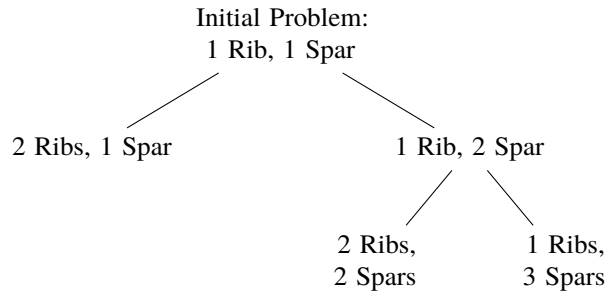
Fig. 1   Example decision tree with configurations as nodes.

A python script, GRASP*, (Guided Rib And Spar Placement) was written to implement the design flow logic and to operate the branch-and-cut algorithm. This design flow is shown in Figure 2; it includes component creation, geometry management and discretization, and the FE analysis.
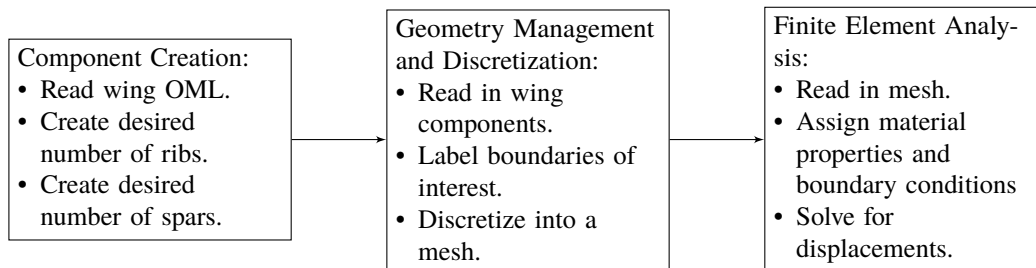
Fig. 2   Automatic design flow logic and steps.

Templated base input files were created for use with each of the subprograms used at each step of the design flow. The python script edited the corresponding input file for the specific problem configuration. It then called each subprogram in the necessary order.

*GRASP repository at github.com/JustinClough/grasp

The script based geometry kernel `Engineering Sketch Pad` (ESP) was used to create a geometry of a problem of interest [18]. For this study, the base geometry was the right wing of the X-15, borrowed from [19]. This geometry was then populated with ribs and spars; these components each had a prescribed thickness. The ribs and spars were written to disk and then read into `Gmsh` [20]. This software then joined all components together through boolean fragmentation and unions to form a single solid geometry. It then was used to produce a second order tetrahedral mesh discretization of this geometry. The FE analysis software `Albany` [21] then read in this mesh, solved a linear elastic problem, and calculated the deformation and stresses of the geometry in the wing under a predefined load condition. Each of these design flow steps are described in detail in the following subsections.

Parametric Geometry with ESP

Two sets of two `.udc` files were written to allow a user to parametrically place ribs and spars for any wing shape. A `.udc` file contains a user defined function. One of these files, `make_rib.udc`, allows the user to place a rib at a specified percent-span. The other in this set is `even_ribs.udc`; this calls `make_rib.udc` to place a user defined number of ribs evenly throughout the span of the wing. A similar set of programs were created for spar placement.

A templated input script was created and used for each problem configuration considered. The numbers of ribs and spars were automatically edited. Next, the ESP binary was called as a subprocess. The geometries created by these scripts were then written to disk as `.stp` files [22]. Each component was written in its own `.stp` file. The generic method was `rib_R.stp` contained all geometric information of rib number R; `spar_S.stp` contained all geometric information of spar number S. When finished, the output was checked for errors.

Three main types of wing shapes were tested to verify the `.udc` files worked as expected. The three wing shapes were Standard, Double Delta, and Double Dihedral. Examples of these shapes are shown in Figure 3.

(a) Standard.   (b) Double Delta.   (c) Double Dihedral.
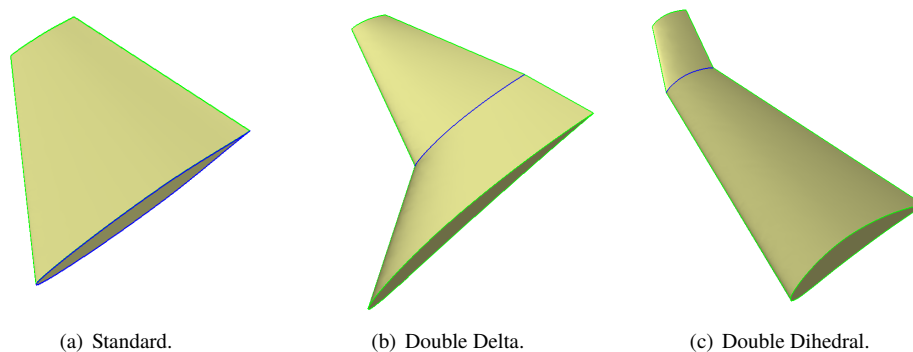
Fig. 3 Geometries of the three base wing types.

The rib and spar file sets were then able to be read into `Gmsh`. The tessellation automatically performed by ESP was not used for the FE analysis.

Geometry Management and Discretization

A template `Gmsh` script file was created and automatically edited for each problem configuration. The script first read the first spar and rib from disk. It then used boolean fragmentation and unions to form a new single continuous volume from the two components. The next component was then read from disk and added to the union in a similar method. This was repeated for all components until a single volume was formed that had all ribs and spars.

Boundaries of interest were then automatically found and labeled. This included the wing root surfaces and the wing underside. Each spar root surface was found by identifying the surface enclosed in a thin bounding box near the wing root and at the corresponding percent chord. The wing underside was determined as the surface with the lowest boundary. These surfaces were labeled such that boundary conditions could be applied during the FE analysis step.

The geometry was then discretized into second order tetrahedral elements. A size field was specified such that at least two elements spanned any geometric feature.

Finite Element Model

Two template `Albany` input files were created and automatically edited for each problem configuration. The first file dictated boundary conditions and linear algebra solver parameters. The second file specified material information such as model type and properties.

A linear elastic material model was used. The user specified the Young's modulus and Poisson ratio for the material. All components of the wing used the same material model and properties. The elements used were 10-node composite tetrahedrons [23]. These elements were chosen after testing in order to ensure that they did not suffer from shear locking often observed in some standard FE formulations.

All degrees of freedom on the wing root surface were assigned a homogeneous Dirichlet boundary condition. The underside of the wing was assigned a Neumann boundary condition of a uniform upward traction. The magnitude of this traction was calculated by distributing a user defined total weight over the lower surface area. This was to represent the lift from airflow over the wing.

Workflow Demonstration

Wing tip deflection was brought below a prescribed allowable level using the `GRASP` program for a example aircraft. The OML of the X-15 was used as the base wing geometry [19]. Material properties of Ti6Al4V were used; these were a Young's modulus of 113.8 GPa and a Poisson's ratio of 0.342 [24]. A weight of 123.0 KN, representing the full weight of the X-15 [19], was distributed uniformly as an upward pressure over the bottom face of the wing. This approximated the load of a 2G maneuver on the wing frame. The spars were created with thicknesses of 30 mm; ribs had a thickness of 5 mm. An allowable tip deflection of 5 cm was used.

Results

Images showing the internal geometries created by the `.udc` files are shown for verification of expected function behavior. This includes internal views for both the Double Delta and Double Dihedral wings. Images and plots from the tip deflection demonstration are presented as well. These include a surface plot tip deflection with respect to considered configurations and images of meshes used for the FE model. Solution times and timing breakdowns are also shown.

Validation of `.udc` Files

The `.udc` files were tested on the Double Delta and Double Dihedral wing types shown in Figure 3. Figure 4 shows the variability of the number of internal components which can be placed. An isometric view of the internal components for the Double Delta wing is shown in Figure 5; a similar view for the Double Dihedral is shown in Figure 6. Images show components with zero thickness for clarity.

(a) Few internal components. (b) Mixed number of internal components. (c) Many internal components.
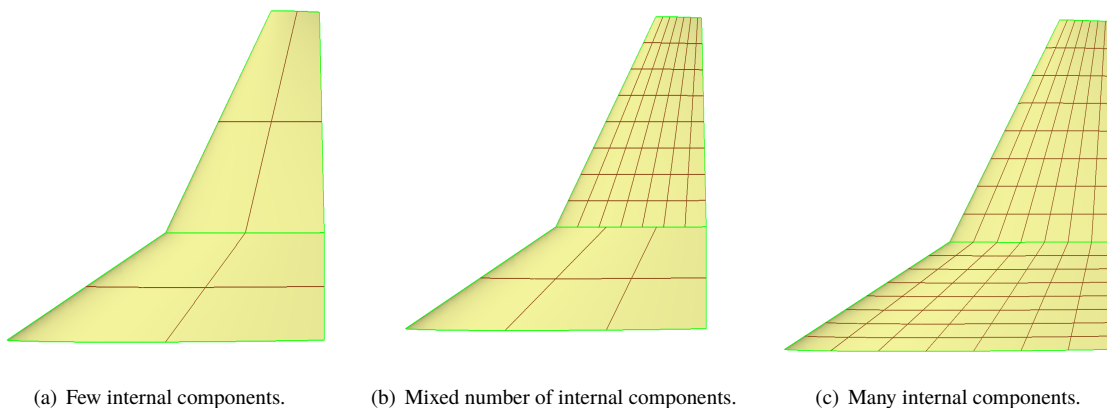
Fig. 4   Double delta wing with differing numbers of parametrically placed internal supports.

(a) External view.

(b) Top surface removed.
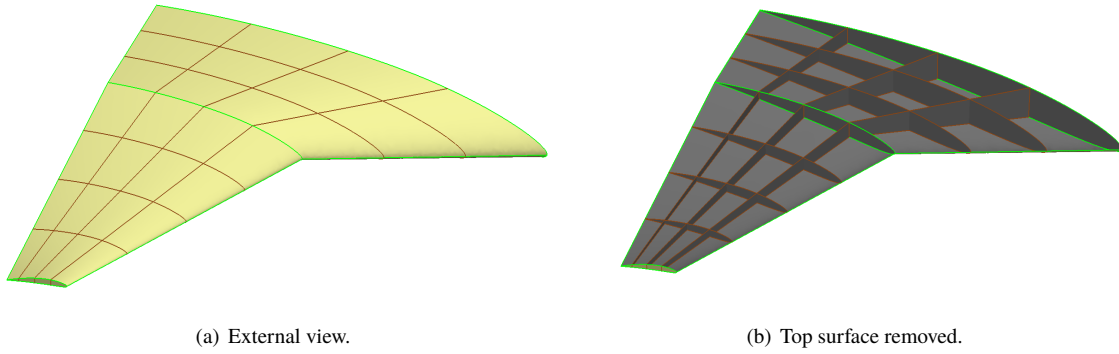
Fig. 5   Double delta wing with and without top surface to show geometries of the internal components.

(a) External view.

(b) Top surface removed.
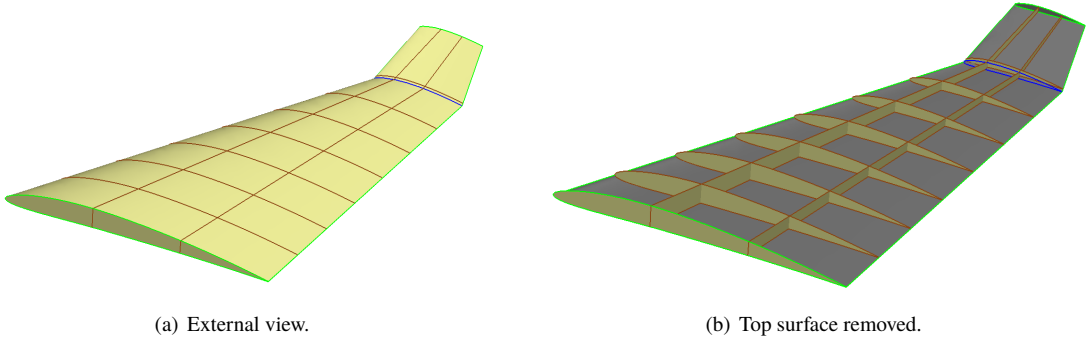
Fig. 6   Double dihedral wing with and without top surface to show geometries of the internal components.

Demonstration Of Full Workflow

   A surface plot generated by computing the tip deflection for numbers of ribs and spars is shown in Figure 7. A spar and rib thickness of 30 mm and 4 mm, respectively, was used along with the geometry and weight for the X-15. This shows the sensitivity of the deflection at the tip of the wing to various configurations of ribs and spars.
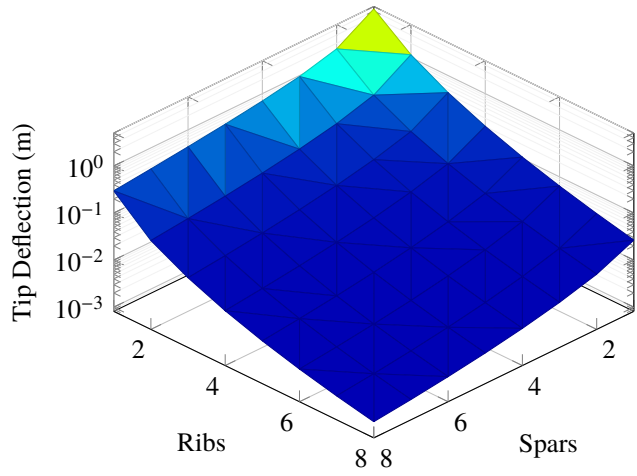
Fig. 7   Tip deflection with respect to numbers of ribs and spars.

6

The maximum tip deflection was for the 1-rib, 1-spar configuration and was 14.6 meters. The minimum tip deflection was 5.9 mm for the 8-rib, 8-spar configuration.

A demonstrative problem was run to test the entire workflow. In this problem the goal was to find the integer combination of ribs and spars that produced a tip deflection for a X-15 wing less than 5 cm with the fewest number of total components. The initial configuration was a wing with a single rib and spar. The skin of the wing was not modeled; it was determined that it did not provide significant bending stiffness to the structure. The entire load on the wing, equal to 123.0 KN, was distributed uniformly on the lower surface of the ribs and spars.

The path selected by the optimization algorithm is shown in Table 1 and Figure 8. The algorithm reached the prescribed constraint in 5 steps. Each step required the generation of two configurations and the solutions of the corresponding structural problems. The final configuration comprised of 5 ribs and 2 spars produced a tip deflection of 3.62 cm. As shown in Figure 8, the algorithm added the second spar in the second step and thereafter always preferred adding a rib over another spar.

Table 1   Intermediate configurations and deflections.

| Step Number	Ribs	Spars	Displacement [mm]
0	1	1	4040.0
1	2	1	966.7
2	2	2	345.5
3	3	2	137.0
4	4	2	66.3
5	5	2	36.2
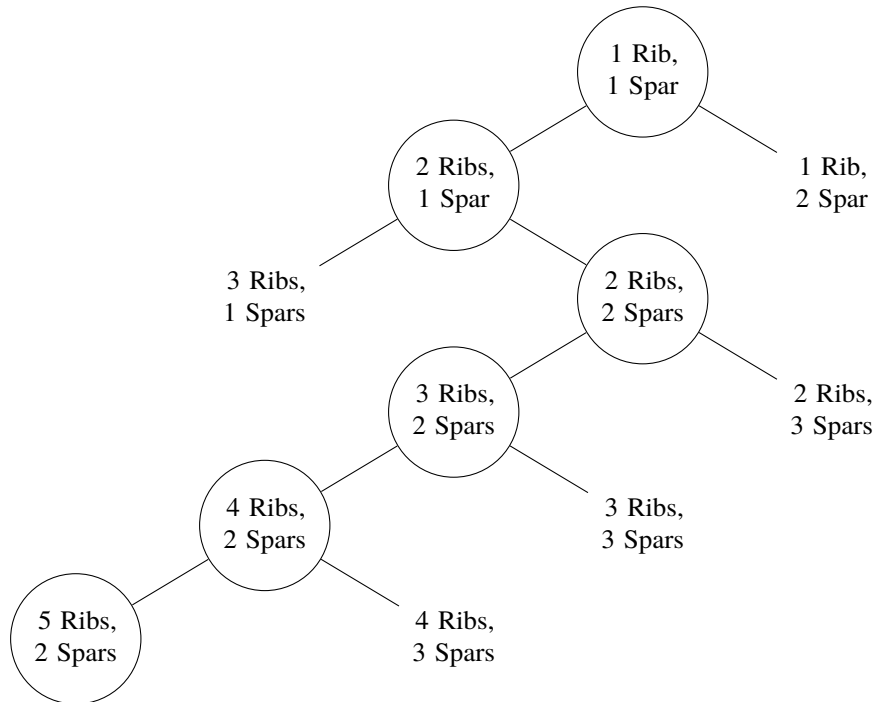
Fig. 8   Path taken by GRASP to build wing frame. Configuration that lowered tip deflection is circled at each level.

The value of tip deflection at each step for the two configurations that were evaluated, one with an extra rib and another with an extra spar, is shown in Figure 9. It was observed that except for the second step, the tip deflection produced by adding an extra rib was smaller than that produced by adding and extra spar.
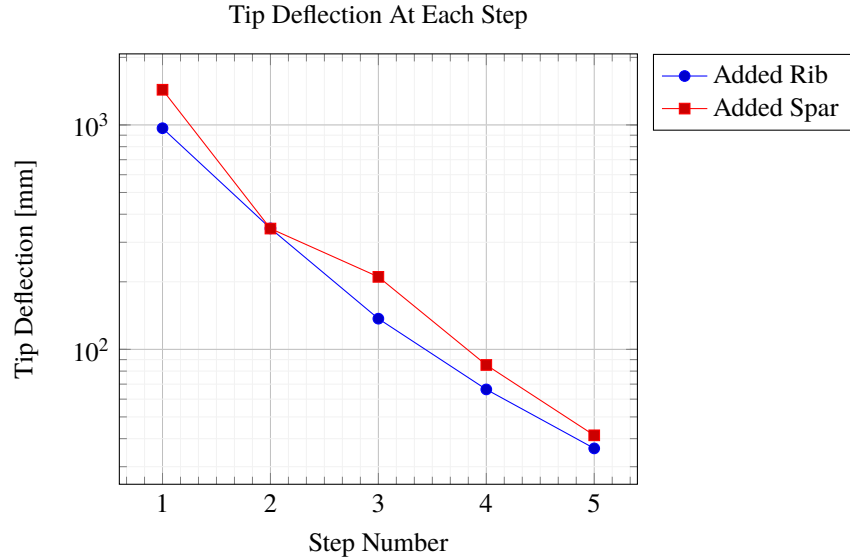
Fig. 9 Tip deflection with respect to the number of steps taken for adding either a rib or spar.

The total computer time required for generating and solving the two configurations at each step is shown in Figure 10. The solution time grows by a factor of 10 between the first and the last step. This is because with each step as more components are added to the model, the effort required to construct and mesh the geometry and then to solve the corresponding FE problem increases. At each step the time required to solve the problem with an extra rib was 21% to 32% more than the time required for the extra spar problem. This can be attributed to the extra effort required in meshing the thin region near the trailing edge. This plot also illustrates the advantage of using the branch-and-cut algorithm over an exhaustive search; spanning the entire parameter space would become prohibitive with the increasing number of components in the latter approach.
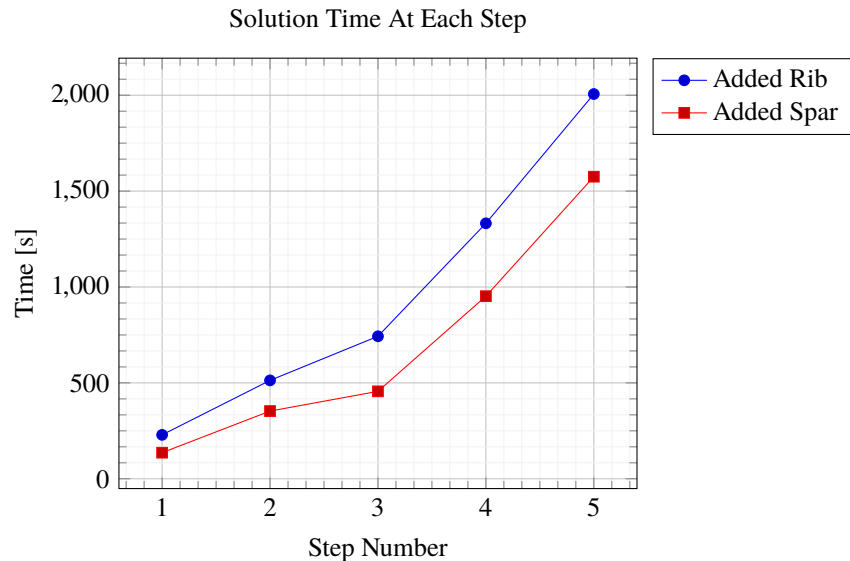
Fig. 10 Time to calculate solution for each configuration with respect to the number of steps taken for adding either a rib or spar.

The number of finite elements generated for the two configurations at each step of the algorithm are shown in Figure 11. These increase by 5,000 to 10,000 with each step and rise to a total of 50,0330 for the final evaluated configuration. On average, spars and ribs required roughly 9000 and 5000 elements to model, respectively.
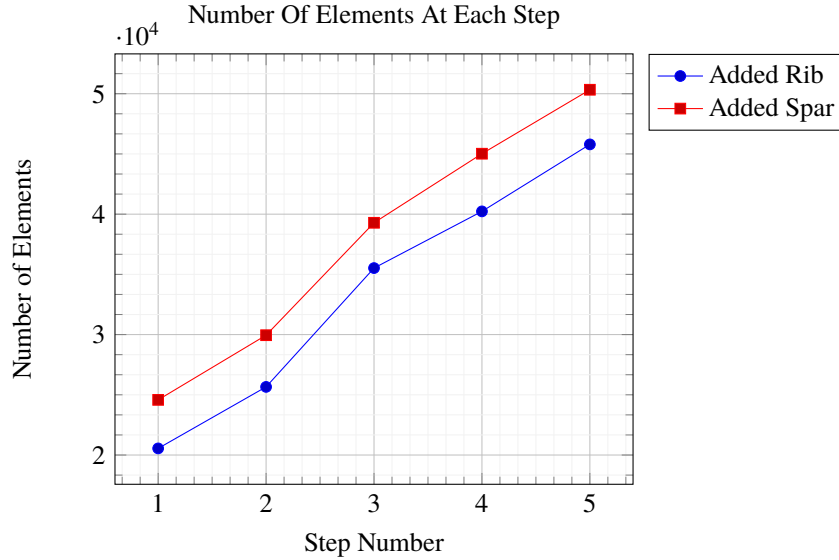
Fig. 11 Finite elements in each mesh for each configuration compared to the number of steps taken for adding either a rib or spar.

Table 2 provides a break-down of the computational time spent in the three main components of the workflow: geometry creation in `ESP`, geometry processing and mesh generation in `Gmsh`, and FE analysis in `Albany`. For the initial configuration, the time spent in `Gmsh` and `Albany` was similar and was three times the time spent in `ESP`. However, for the final few configurations the situation was reversed; here most of the time was spent in combining the different components and then meshing them in `Gmsh`. Remarkably the time required for the FE analysis was less than a tenth of this time. This may be attributed to the advanced solvers and preconditioners used within `Albany` [21]. The program took a total of 139 minutes to run on a Linux workstation with a i5-7400 CPU which had a clock speed of 3 GHz.

Table 2 Time in each portion of the design flow throughout evaluated configurations. All times in seconds.

| Step Number	Ribs	Spars	Geometry Creation	Geometry Management and Discretization	FE Analysis
0	1	1	13	39	39
1	2	1	14	66	89
2	2	2	14	287	69
3	3	2	16	656	91
4	4	2	16	1206	112
5	5	2	16	1871	122

In Figure 12, the geometry and the mesh at each step are plotted; in Figure 13 the deformed shape of the configuration is shown. In this figure, for each configuration, the surface is colored with the magnitude of displacement. The maximum deflection occured at the tip of the spar closer to the leading edge, and that with each new rib that was added the magnitude of this displacement, as well as the difference between the tip deflection of this spar and the one downstream of it, reduced.
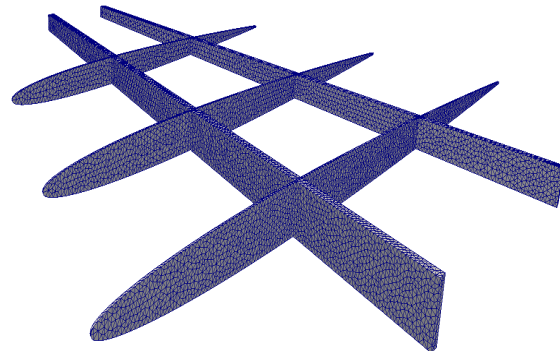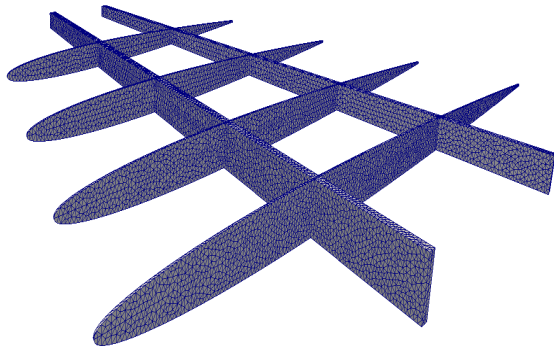
9
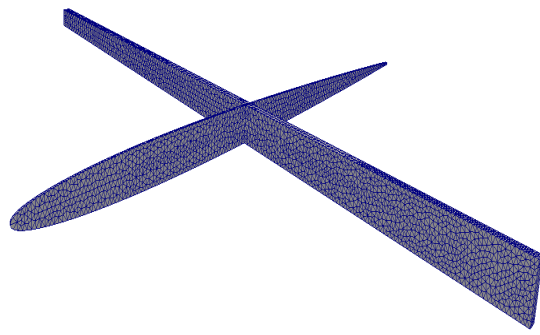
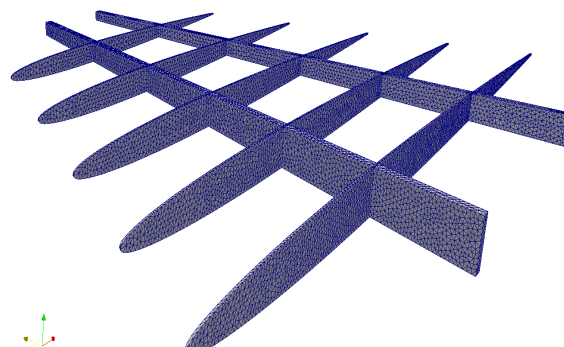(a) Step 0: 1 Rib, 1 Spar.
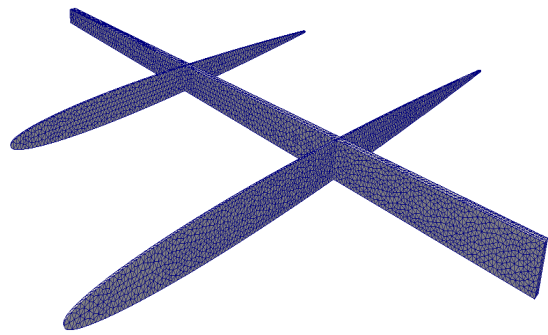
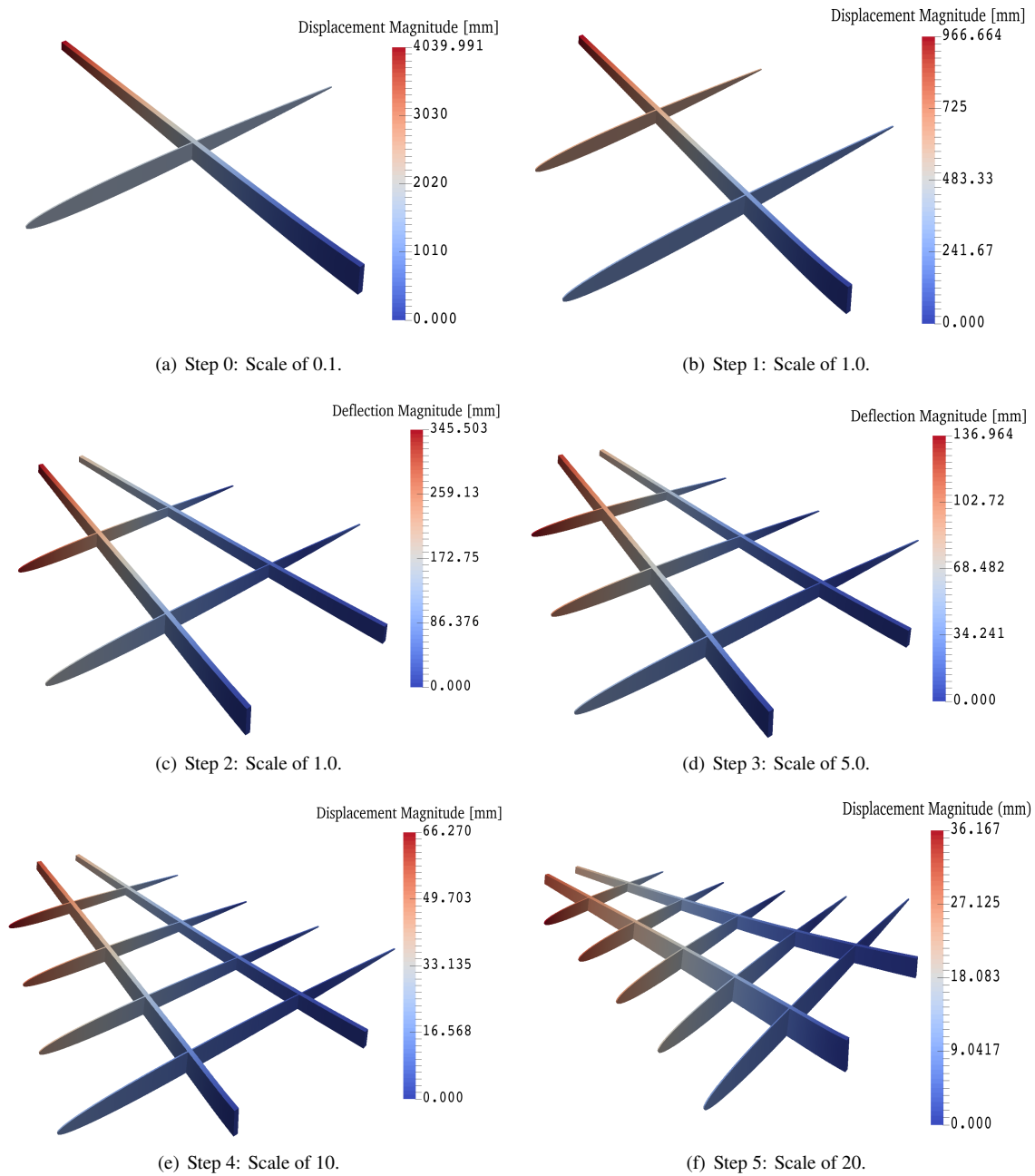(b) Step 1: 2 Rib, 1 Spar.
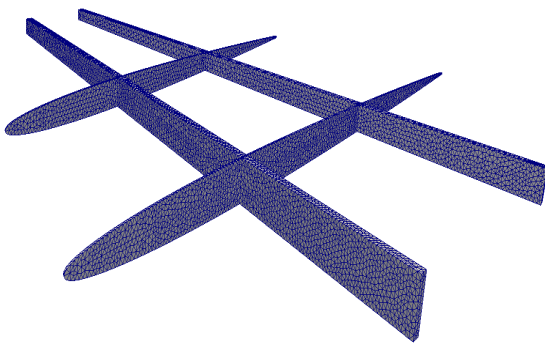
(c) Step 2: 2 Rib, 2 Spar.

(d) Step 3: 3 Rib, 2 Spar.

(e) Step 4: 4 Rib, 2 Spar.

(f) Step 5: 5 Rib, 2 Spar.

Fig. 12   Meshes used at different solution steps.

(a) Step 0: Scale of 0.1.

(b) Step 1: Scale of 1.0.

(c) Step 2: Scale of 1.0.

(d) Step 3: Scale of 5.0.

(e) Step 4: Scale of 10.

(f) Step 5: Scale of 20.

Fig. 13 Mesh at each step with displacement magnitude contour plot and deformed with the displacement vector; scale factors used to show deflections.

Discussion and Closing Remarks

The GRASP program was able to solve an optimal parametric structural layout problem by automatically creating an initial frame design. A user specified design constraint, maximum allowable wing deflection, was satisfied by determining the integer numbers of ribs and spars to populate the wing frame for a demonstrated vehicle. A simplified version of the branch-and-cut method was used to step through possible configurations. For each configuration, a design flow consisting of component creation, geometry discretization, and a FE analysis was executed.

The components of the wing frame were created using the parametric, script-based, geometry kernel ESP. Each

component was written to disk and then read into `Gmsh` automatically. The components were then unioned together to form one continuous volume which represented the wing frame. Boundaries of interest were tagged and the volume was discretized into a FE mesh which was written to disk. This mesh was then read into `Albany` where boundary conditions and material properties were assigned. The FE problem was then solved for nodal displacements.

The demonstration shows that the `GRASP` program was able to create a design for the frame of a wing OML automatically in approximately 2 hours. In this time it considered 11 different configurations and successively chose the one which lowered tip deflection. This was done using all open-source software packages.

This work demonstrates a viable method to bring structural layout into the initial design phase for aircraft. It does so without the need for a structural design specialist present. This will benefit the air vehicle design community by introducing greater modeling accuracy earlier in the design process. In turn this will lead to aircraft designs which more efficiently meet their design criteria. Additionally, layouts generated using `GRASP` rely on traditional and tested manufacturing methods.

Future Work

Possible improvements would include allowing for different materials throughout the wing, modeling the wing skin with stringers, and testing under more load cases. These additions would allow for more accurate modeling of the wing in use.

Allowing for different components to have different material properties would generalize the given method. Some but not all wing constructions use the same material throughout the wing. For example, the X-15 used both Inconel and Titanium alloys in its wing construction, [25, 26], whereas a commercial Cessna uses the same Aluminum alloy throughout the wing, only differing by temper [27]. Additionally, different material models could be used on different components. These models would include the pertinent physical behavior needed to understand the performance of the design. Including the wing skin and stringers would also increase the general accuracy of the model. This would be especially important for more complex load cases where the stringers and skin must distribute the aerotractions to the ribs and spars. Lastly, more complex load cases could be created and designed for to better represent those in flight.

The `GRASP` software can also be made faster by a few methods. First, configurations can be processed in parallel; this would decrease the total solution time to near half. Second, both `Gmsh` and `Albany` are able to operate in parallel [20, 21]. Calling these application with parallel resources would also decrease the time to solve each configuration. Finally, each step of the design flow shown in Figure 2 starts and end with reading a writing to the disk. Processing fully in memory without the file input/output would also decrease the total time to calculate solutions.

Acknowledgments

References

[1] Horvath, B. L., "Aircraft Conceptual Structural Design Using The AMMIT Structural Analysis Tool," AIAA Scitech 2019 Forum, 2019.

[2] Alyanak, E., and Kolonav, R., "Efficient Supersonic Air Vehicle Structural Modeling For Conceptual Design," 12th AIAA Aviation Technology, Integration, and Operations Conference and 14th AIAA/ISSMO Multidiciplinary Analysis and Optimization Conference, 2012.

[3] Sensmeier, M., and Samareh, J., "Automatic Aircraft Structural Topology Generation For Multidisciplinary Optimization and Weight Estimation," 46th AIAA/ASME/ASCE/AHS/ASC Structures, Structural dynamics and Materials Conference, 2005.

[4] Saitao, K., Izui, K., Nishiwaki, S., and Papalambros, P., "A Survey of Structural Optimization in Mechanical Product Development," Transactions of the ASME, Vol. 5, 2005.

[5] Brampton, C., Kim, H., and Cunningham, J., "Level Set Topology Optimization of Aircraft Wing Considering Aerostructural Interaction," 12th AIAA Aviation Technology, Integration, and Operations Conference and 14th AIAA/ISSMO Multidiciplinary Analysis and Optimization Conference, 2012.

[6] Frazier, W. E., "Metal Additive Manufacturing: A Review," Journal of Materials Engineering and Performance, Vol. 23, No. 6, 2014.

[7] Uriondo, A., Esperon-Miguez, M., and Perinpanayagam, S., "The present and future of additive manufacturing in the aerospace sector: A review of important aspects," Proceedings of the Institution of Mechanical Engineers, Part G: Journal of Aerospace Engineering, Vol. 229, No. 11, 2015, pp. 2132–2147.

[8] Wong, K. V., and Hernandez, A., "A Review of Additve Manufacturing," International Scholarly Research Network: Mechanical Engineering, Vol. 2012, 2012.

[9] Mason, B. H., and Quinlan, J., "Conceptual Design Shop: A Tool for Rapid Airframe Structural Modeling," 2018 AIAA/ASME/AHS/ASC Structures, Structural Dynamics, and Materials Conference, 2018.

[10] Hwang, J., Kenway, G., and Martins, J., "Geometry And Structural Modeling For High-Fidelity Aircraft Conceptual Design Optimization," 15th AIAA/ISSMO Multidisciplinary Analysis and Optimization Conference, 2014.

[11] Padula, S., Robinson, J., and Eldred, L., "Structural Analysis In A Conceptual Design Framework," 53rd AIAA/ASME/ASCE/AHS/ASC Structures, Structural Dynamics and Materials conference, 20th AIAA/ASME/AHS Adaptive Structures Conference, 14th AIAA, 2012.

[12] lazzara, D., Parham, J., and Haimes, R., "On Structural Layout Using Multifidelity Geometry in Aircraft Conceptual Design," 48th AIAA Aerospace Sciences Meeting including the New Horizons Forum and Aerospace Exposition, 2010.

[13] Bryson, D., Rumpfkeil, M., and Durscher, R., "Framework for Multifidelity Aeroelastic Vehicle Design Optimization," 18th AIAA/ISSMO Multidisciplinary Analysis and Optimization Conference, 2017.

[14] Padberg, M., and Rinald, G., "A Branch-And-Cut Algorithm For the Resolution Of Large-Scale Symmetric Traveling Salesman Problems," Society for Industrial and Applied Mathematics Review, 1991.

[15] Anemaat, W. A., Kaushik, B., Hale, R. D., and Ramabadran, N., "AAARaven: Knowledge-Based Aircraft Conceptual and Preliminary Design," 48th AIAA/ASME/ASCE/AHS/ASC Structures, Structural Dynamics, and Materials Conference, 2007.

[16] Niu, C., "Airframe Structural Design: Practical Design Information and Data on Aircraft Structures," Hong Kong: Conmilit Press Limited, 1999.

[17] Sensmeier, M., and Samareh, J., "A Study Of Vehicle Structural Layouts In Post-WWII Aircraft," 45th AIAA/ASME/ASCE/AHS/ASC Structures, Structural Dynamics and Materials Conference, 2004.

[18] Haimes, R., and III, J. F. D., "The Engineering Sketch Pad: A Solid-Modeling, Feature-Based, Web-Enabled System for Building Parametric Geometry," Fluid Dynamics and Co-located Conference: 21st AIAA Computational Fluid Dynamics Conference, 2013.

[19] Gochenaur, D., "Rapid Geometry Generation and Basic Comparison of Aerodynamic Performance Using the X-15 Hypersonic Test Vehicle," Internal Report, 2017.

[20] Geuzaine, C., and Remacle, J.-F., "Gmsh: A Three-Dimensioal Finite Element Mesh Generator With Generator With Bruild-In Pre- and Post-processing Facilities," International Journal For Numerical Methods In Engineering, Vol. 79, 2009.

[21] Salinger, A. G., Bartless, R. A., Bradley, A. M., Chen, Q., Demeshko, I. P., Gao, X., Hansen, G. A., Mota, A., Muller, R. P., Nielsen, E., Ostien, J. T., Pawlowski, R. P., Perego, M., Phipps, E. T., Sun, W., and Tezaur, I. K., "Albany: using Component-Based Design To Develop A Flexible, Generic Mulitphysics Analysis Code," International Journal For Multiscale Computaional Engineering, Vol. 14, No. 4, 2016.

[22] Mayes, R., Swope, K., Mathew, L., and Stanton, B., "ISO 10303-21:2016: Industrial Automation Systems and Integration-Product Data Representation And Exchang-Part 21: Implementation Methods: Clear Text Encoding Of The Exchange Strcuture," International Organization for Standardization Catalogue, Vol. 21, 2016.

[23] Ostien, J. T., Foulk, J. W., Mota, A., and Veileux, M. G., "A 10-Node Composite Tetrahedral Finite Element For Solid Mechanics," International Journal For Numerical Methods In Engineering, Vol. 107, 2016.

[24] Boyes, R., Welsch, G., and Collings, E., "Materials Properties Handbook: Titanium Alloys," ASM International, 1994.

[25] Kordes, E. E., Reed, R. D., and Dawdy, A. L., "Structural Heating Experiences On The X-15 Airplane," National Aeronautics and Space Administration: Technical Memorandum, 1962.

[26] Price, A. B., "Design Report-Thermal Protection System X-15A-2," National Aeronautics and Space Administration: Technical Memorandum, 1968.

[27] Company, C. A., Maintenance Manual: Single Engine Models 172, 182, T182, 206 and T206 1996 And On, PO Box 7706, Wichita, KS 67277-7706, 4th ed., 6 2005.